

Experimental Identification of Electromagnetically Induced Transparency in Magnetized Plasma

Eiichirou Kawamori,¹ Wun-Jheng Syugu,² Tung-Yuan Hsieh,¹ Sung-Xuang Song,¹ and C. Z. Cheng³

¹*Institute of Space, Astrophysical and Plasma Sciences, National Cheng Kung University, Tainan 70101, Taiwan*

²*Department of Physics, National Cheng Kung University, Tainan 70101, Taiwan*

³*Plasma and Space Science Center, National Cheng Kung University, Tainan 70101, Taiwan*

(Received 2 October 2011; published 17 February 2012)

We report the first experimental identification of the new wave branch at electron cyclotron frequency produced by the injection of a frequency-matched intense pump wave in magnetized plasma [A. G. Litvak and M. D. Tokman, *Phys. Rev. Lett.* **88**, 095003 (2002); G. Shvets and J. S. Wurtele, *Phys. Rev. Lett.* **89**, 115003 (2002)], which is a classical phenomenon analogous to electromagnetically induced transparency (EIT) in quantum systems. By using a frequency-sweep interferometer, we directly detected the dispersion relation of the plasma EIT branch for propagation parallel to the background magnetic field. The bandwidth of the EIT window was correlated with the pump-wave electric field and was found to agree with the theoretical prediction.

DOI: 10.1103/PhysRevLett.108.075003

PACS numbers: 52.35.Mw, 52.25.Xz, 52.35.Hr

Electromagnetically induced transparency (EIT) in quantum atomic systems is a phenomenon in which optical properties of matter, such as absorption and emission, are drastically altered as a result of quantum interference between eigenstates of matter when irradiated with two optical fields [1]. In other words, the susceptibility and permittivity of a medium can be manipulated by controlled laser light. EIT is the basis of several applications such as slow light [2], information transfer between matter and light [3], and lasing without inversion [4].

Harris theoretically proposed using plasma as a medium for EIT [5]. Subsequently, new plasma EIT for electron cyclotron waves in magnetized plasma was proposed by researchers including Litvak and Shvets [6,7]. Their theories predict that the injection of a tuned pumping wave alters the susceptibility of plasma to right-hand circularly polarized (RHCP) electron cyclotron waves. As a result, RHCP waves no longer resonate with electrons at the electron cyclotron frequency, and plasma becomes transparent to RHCP waves.

It is noted that the EIT in plasmas is a classical analogous phenomenon to the quantum EIT and does not invoke quantum mechanics while it is key essential to the conventional EIT. EIT in plasmas is achieved by the coupling of collective oscillations of a medium rather than the destructive interference of quantum states. In particular, in the EIT of an RHCP wave, cancellation of the polarization current by the coupling of longitudinal plasma oscillation with the pump-induced motion of electrons allows EIT-band creation when the system satisfies the matching condition of $f_{\text{probe}} \approx f_{\text{ce}} \approx f_{\text{pump}} + f_{\text{pe}}$, where f_{probe} , f_{ce} , f_{pump} and f_{pe} the probe-wave frequency, the electron cyclotron frequency, the pump-wave frequency, and the plasma frequency, respectively. Litvak and Shevets elucidated that the RHCP-wave group velocity depends on the pump-wave intensity [6,7]. This dependence enables

extremely slow propagation of the RHCP wave packet and leads to many potential applications.

The EIT in magnetized plasmas has a variety of potential applications including the energy compression of electromagnetic microwaves [8], ion acceleration by the ponderomotive force, and the control of the spatial absorption profile of electron cyclotron heating (ECH) waves in fusion plasmas [9]. Although many theories and numerical studies have been reported [10,11], experimental studies on the EIT in magnetized plasma have not yet been conducted. This Letter presents the first experimental observation of the EIT in magnetized plasma.

To simplify the experimental conditions for identifying the EIT branch, we prepared a uniform one-dimensional plasma. According to the theory, the EIT branch is expected to appear at the electron cyclotron frequency band in the ω - k_{\parallel} space when the pump wave is injected. Figure 1 shows a schematic of the experimental setup. The magnetic mirror device, MPX [12] generated a cylindrical plasma with a diameter of ~ 15 cm. In this experiment,

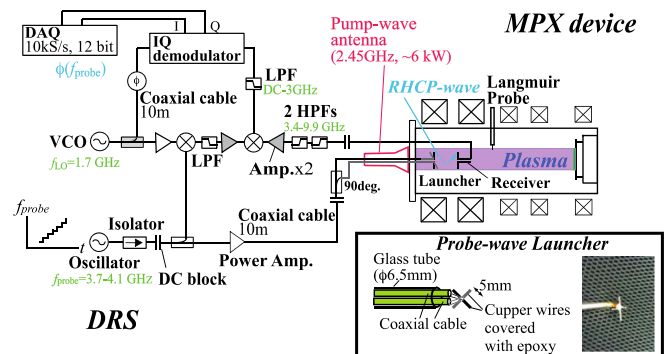


FIG. 1 (color online). The schematic of experimental setup including dispersion-relation scanner (DRS) and the magnetized plasma experiment (MPX) device.

argon plasmas were produced by electron cyclotron resonance (ECR) discharge. We utilized a magnetron oscillator, whose frequency and maximum net output power are 2.45 GHz and about 6 kW, respectively, as a plasma generator for ECR discharge and a pump-wave source for EIT. A pump wave was injected into the MPX plasma along the background magnetic field lines from an endplate of the vacuum chamber through a waveguide and a glass window. The wave launched to produce the plasma was a linear polarized mode.

The electron density measured with a Langmuir probe was $1\text{--}5 \times 10^{16} \text{ m}^{-3}$ throughout the experiment. The electron temperature in this experiment was 3–10 eV ($\pm 2\text{--}5$ eV). The fill pressure of the argon gas was ~ 0.5 mTorr. The Debye length was about 0.1–0.2 mm. The electron mean free path for electron-ion collisions was of the order of 10 meters and for electron-neutral collisions was larger than 1 m. The background magnetic field at the position where the EIT-branch dispersion relation was measured was about 0.133–0.136 T. The electron cyclotron resonance layer for ECR discharge (at where field strength was ~ 0.089 T) was positioned ~ 60 cm downstream of the measurement location with respect to the endplate.

To obtain the probe-wave dispersion relation in the magnetized plasma at the electron cyclotron frequency band, we employed a dispersion-relation scanner (DRS), which is a frequency-sweep interferometer. A schematic of DRS is given in Fig. 1. DRS generated microwaves (probe waves) with a main oscillator and launched them through amplifiers, coaxial cables, and dipole antennas. A set of two antennas was immersed in the plasma to launch the RHCP probe wave in the plasma by combining a sinusoidal wave and 90° -delayed wave. Each antenna was 5 mm in length and was coated with thin vacuum-use epoxy (Torrseal). A photograph of the antenna launcher is shown in Fig. 1.

The probe-wave with power of ~ 1 W excited by the launcher propagated along the magnetic field lines and was received by another antenna. The received microwave was passed through two high-pass filters to prevent the high-power pump wave from reaching the detection circuit of DRS. A balanced mixer down-converts frequency of the received probe wave to that of the local oscillator (1.7 GHz).

An inphase-quadrature (I-Q) demodulator extracted information regarding the phase difference between the reference wave obtained from the transmission line of the main oscillator and the received probe wave. The output of the I-Q demodulator was acquired using a digitizer (DAQ). The wave number k was calculated from the relationship $k = \phi/d$, where ϕ is the phase difference and d is the distance between the launcher and receiver antennas. This relationship is valid when the Wentzel-Kramers-Brillouin (WKB) condition (geometric optics condition) is satisfied.

Because the main oscillator scanned the probe-wave frequency from 3.7 GHz with a frequency step of 400 kHz, DRS could give the relationship between ω and k : that is, a dispersion relation for an RHCP mode in the magnetized plasma. The distance d between the launching antenna and the receiver antenna was chosen such that the received probe wave satisfied the far-field condition. In general, the far-field condition is given as $d \geq \lambda/(2\pi)$, where λ is the wavelength of the probe wave. Moreover, the shorter d is, the better is the homogeneity of the plasma parameters. In fact, we directly confirmed the far-field condition from the measurement of the IQ signal by using a phase shifter in vacuum.

The experimental condition satisfied the WKB condition with $d = 1.5$ cm such that $(\frac{1}{B_{z0}} \frac{\partial B_{z0}}{\partial z})^{-1} \sim 0.135 [\text{T}] \times 0.1 [\text{m}] / 0.003 [\text{T}] = 4.5 [\text{m}] \gg d = 0.015 [\text{m}]$, where B_{z0} is the background magnetic field strength.

Frequency of the probe wave was scanned with a frequency step Δf_{probe} of 400 kHz. The pulse width of the probe wave for each frequency component was 1.0 ms and the interval between the pulses was 0.3 ms. The pulse width and interval were determined to make it possible to distinguish the respective responses of the plasma to the probe-wave injection from the respective frequency components. For calibration, reference data of the I-Q measurement (such as the center of the I-Q circle, the initial phase information and so on) were taken before each plasma-shot under the vacuum condition.

The I-Q-signal phase change ϕ and the effective transmittance of probe wave are plotted as a function of probe-wave frequency f_{probe} in Fig. 2. The effective transmittance was evaluated as $(E_{\text{plasma}}/E_{\text{vacuum}})^2$, where E_{plasma} and E_{vacuum} are the probe-wave electric fields in the plasma and in vacuum obtained from the amplitude of the In- and quadrature signals. The results correspond to the cases of pump-wave power $P_{\text{pump}} = 2.8$ kW and 5.2 kW, respectively. In both cases, as f_{probe} approached 3.75 GHz, ϕ sharply increased. Note that the transmittance also decreased as f_{probe} approached 3.75 GHz, which corresponded to the electron cyclotron frequency f_{ce} in both cases. Therefore, we consider that the decrease in the effective transmittance corresponds to ECR.

In each case of the different pump powers in Fig. 2, the effective transmittance for f_{probe} from 3.750 to 3.765 GHz is expanded to the right-side box. In the case of $P_{\text{pump}} = 2.8$ kW, the effective transmittance was smaller than unity when $f_{\text{probe}} > 3.756$ GHz. This corresponds to the stop band between ECR and the right-hand cutoff frequency $f_{\text{RH}} = 4.1$ GHz. However, in the case of $P_{\text{pump}} = 5.2$ kW, the transmittance exceeded unity again at around $f_{\text{probe}} = 3.762$ GHz, which indicates the EIT branch.

Figure 3 shows the dispersion relation (f_{probe} vs k) for the probe wave for different pump powers P_{pump} of 2.8, 4.7, and 5.2 kW. Only k for which the effective transmittance is

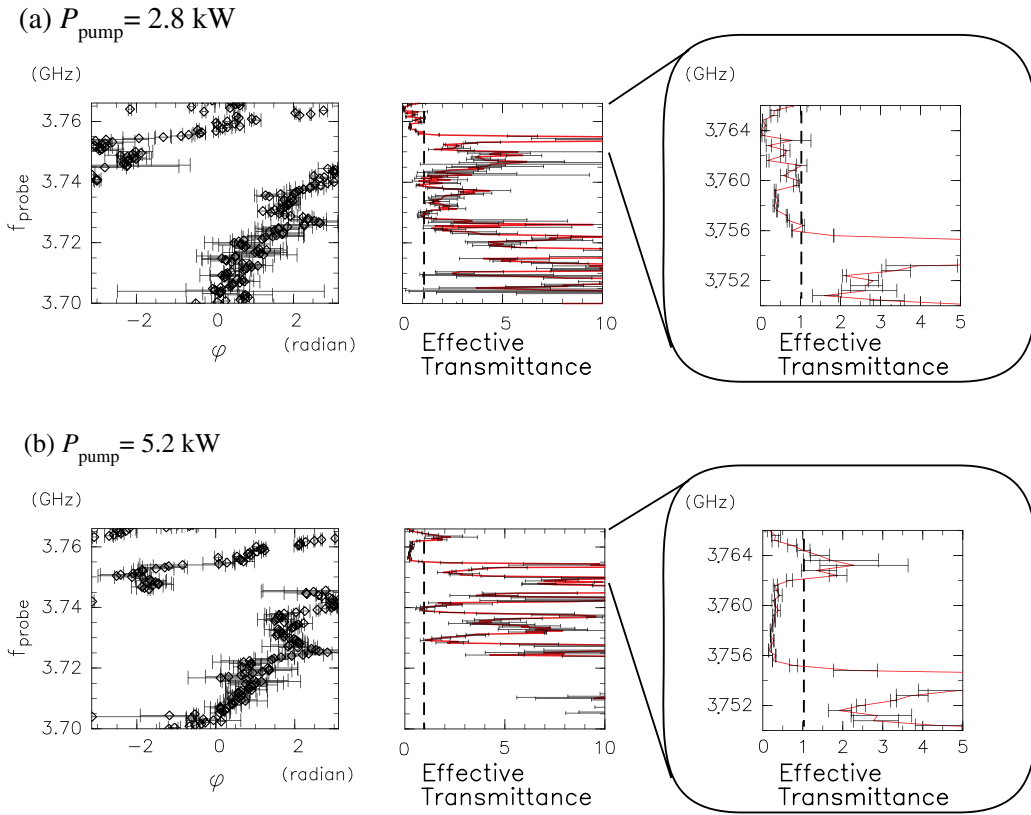


FIG. 2 (color online). I-Q-signal phase change ϕ and effective transmittance of the probe wave are plotted as a function of the probe-wave frequency f_{probe} .

larger than unity is plotted for f_{probe} under the assumption that a lower value of the effective transmittance indicates lower correlation between the probe and reference waves. Theoretical dispersion relations of RHCP waves including the EIT branch, left hand circularly polarized (LHCP) wave and light in vacuum are plotted together with the experimental data. The horizontal error bars in Fig. 3 represent the error of the phase measurement, which is evaluated from the signal-to-noise ratio of the IQ signal and contamination by the LHCP-wave power in the IQ detection since the LHCP wave had a wave branch at this

frequency band as well. The contamination by the LHCP-wave power contributes to the phase error $\Delta\phi$ as $\Delta\phi = [\arctan\{(P_{\text{LH}}/P_{\text{RH}})\}^{1/2}]$ in the case of $P_{\text{LH}} \leq P_{\text{RH}}$ at maximum, where P_{RH} and P_{LH} are the RHCP-wave and LHCP-wave powers detected by DRS. In Fig. 3, we assume $P_{\text{LH}} = P_{\text{RH}}$. This assumption overestimates the error by a factor of about five at maximum.

The measurement data points for f_{probe} below 3.75 GHz deviate from the branches of light in vacuum and LHCP wave, which are shown by gray and blue dotted lines and agree well with the low-frequency R-mode branch (shown

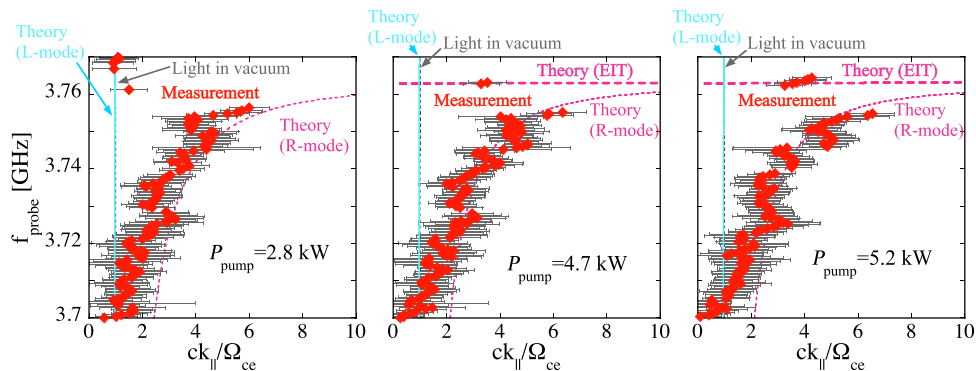


FIG. 3 (color online). Dispersion relation of the probe wave for different pump powers P_{pump} of 2.8, 4.7, and 5.2 kW.

by dotted pink curves) of the cold plasma dispersion relation with $n_{e0} = 1.5 \times 10^{16} \text{ m}^{-3}$ for all values of P_{pump} . This density corresponds to $0.84f_{\text{pe}}^{\text{EIT}}$, where $f_{\text{pe}}^{\text{EIT}}$ is the density required for perfect matching condition of the EIT $f_{\text{probe}} \approx f_{\text{pump}} + f_{\text{pe}}^{\text{EIT}}$. A new branch appeared above the low-frequency *R*-mode branch when P_{pump} reached 4.7 kW. The window of the new branch Δf_{EIT} was wider and clearer for $P_{\text{pump}} = 5.2 \text{ kW}$ than for $P_{\text{pump}} = 4.7 \text{ kW}$. These newly appearing branches agree well with the theoretical prediction by Ref. [6], which are shown by the dotted pink curves.

Figure 4(a) shows the relationship between the bandwidth Δf_{EIT} of the EIT branch and P_{pump} . By fitting a line to the experimental data points, we estimate that the threshold of P_{pump} to form the EIT band is 4.5 kW. In Fig. 4(b), we calculate the normalized electric field of the pump wave by using the threshold power $P_{\text{pump}}^{\text{threshold}}$ as follows:

$$\xi \equiv \frac{eE_{\text{pump}}}{m_e \omega_{\text{pump}} c},$$

$$P_{\text{pump}} - P_{\text{pump}}^{\text{threshold}} = \frac{\varepsilon |E_{\text{pump}}|^2}{2} v_g^{\text{pump}} A,$$

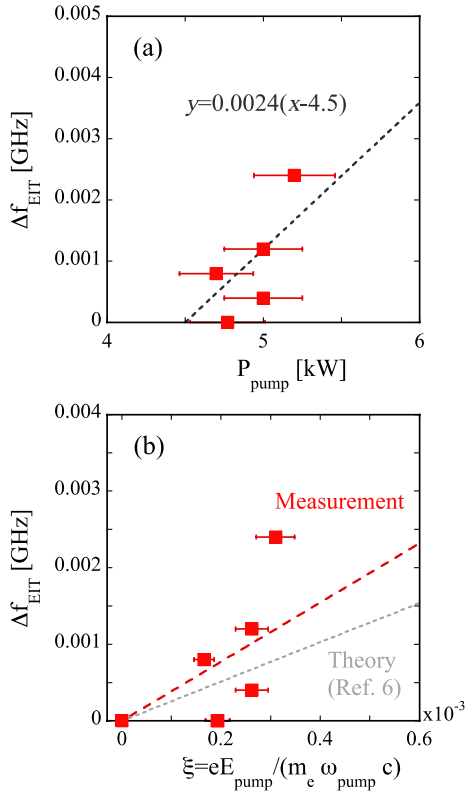


FIG. 4 (color online). (a) Relationship between the bandwidth Δf_{EIT} of the EIT branch and pump-wave power P_{pump} and (b) relationship between the bandwidth Δf_{EIT} of the EIT branch and normalized pump-wave electric field ξ .

where ε , v_g^{pump} and A are the permittivity of the plasma, the pump-wave group velocity calculated from the cold plasma dispersion relation (CPDR) and the cross-sectional area of the pump wave, respectively.

In Fig. 4(b), we find that the measurement agrees with the theoretical prediction of the effective Rabi frequency (dotted line) given by Shvets and Wurtele [6], despite the measured data being somewhat scattered and the slope of the line for the measured Δf_{EIT} vs ξ being larger than that of the theoretical line.

Possible reasons to explain this discrepancy between measurement and theory include effects that are not considered by the theory, such as thermal motion of electrons. According to the fluid theory of warm plasma-EIT [11], thermal effect of the electrons makes the EIT branch split into two branches as a result of change in the longitudinal plasma oscillation, which modifies the EIT matching condition as $(\omega_{\text{probe}} - \omega_{\text{pump}})^2 \approx \omega_{\text{pe}}^2 + 3(k_{\text{probe}} - k_{\text{pump}})^2 \times (k_B T_e / m_e)$. This split expands apparent band width of the EIT Δf_{EIT} . In our plasma, although the electron temperature was small to modify the matching condition ($\because (\omega_{\text{probe}} - \omega_{\text{pump}})^2$ or $\omega_{\text{pe}}^2 \gg 3(k_{\text{probe}} - k_{\text{pump}})^2 \times (k_B T_e / m_e)$), it might have expanded Δf_{EIT} from that predicted by the cold plasma EIT theory because the term pertinent to the warm plasma effect $3(k_{\text{probe}} - k_{\text{pump}})^2 \times (k_B T_e / m_e)$ (\sim a few MHz) was comparable to the effective Rabi frequency $\Omega_R \approx \Delta f_{\text{EIT}}$. In addition, the significant inaccuracy of the n_{e0} measurement might have caused a certain amount of frequency mismatch in the requirement for EIT, which may lead to data scattering. We speculate that a frequency mismatch of $0.7f_{\text{pe}}^{\text{EIT}} - 1.5f_{\text{pe}}^{\text{EIT}}$ could lead to a decrease in Δf_{EIT} by a few tens percents. Uncertainties of this magnitude do not alter the main conclusions of this work but we are continuing to investigate this relationship. It is considered that narrow EIT-band width Δf_{EIT} due to the small pump power made the decay length of the probe waves being considerably short (by resonant absorption). This considerably short decay length might have been a cause of the data scattering.

In conclusion, we have reported the first experimental identification of the EIT-created RHCP-wave branch in magnetized plasma. By using a frequency-sweep interferometer, we directly detected the dispersion relation of the EIT branch. The new wave branch appeared in the frequency band between the original electron cyclotron frequency and the right-hand cutoff frequency. The bandwidth of the EIT window was correlated with the electric field of the pump wave, and the results were consistent with theoretical predictions.

For the EIT probe wave with a finite pulse width, a wide bandwidth of the EIT window is necessary because the pulsed probe wave contains frequency components with finite bandwidth. Therefore, large pump-wave power is required for the transparency of a pulsed probe wave. According to the physics of dark-state polaritons for the

EIT in magnetized plasma [13], which is analogous to that in cold atomic systems [14], a pulsed pump wave properly controlled in time domain can slow down propagation of a probe-wave packet in a short time period with realistic power. This scenario may lead to an EIT ion accelerator. Therefore, this work is an essential step for such future applications.

The authors would like to thank Professor Yasuhi Nishida of National Cheng Kung University and Professor Atushi Mase of Kyusyu University for stimulating and encouraging discussions. The authors are grateful to the members of the MPX group of Plasma and Space Science Center of National Cheng Kung University for their contributions to this study. This work was supported by Grants-in-Aid 97-2112-M-006-016-MY3 from the National Science Council of Taiwan.

-
- [1] K.J. Boller, A. Imamoglu, and S.E. Harris, *Phys. Rev. Lett.* **66**, 2593 (1991).
 - [2] L.V. Hau, S.E. Harris, Z. Dutton, and C.H. Behroozi, *Nature (London)* **397**, 594 (1999).

- [3] M. Fleischhauer, S.F. Yelin, and M.D. Lukin, *Opt. Commun.* **179**, 395 (2000).
- [4] A.S. Zibrov, M.D. Lukin, D.E. Nikonov, L. Hollberg, M.O. Scully, V.L. Velichansky, and H.G. Robinson, *Phys. Rev. Lett.* **75**, 1499 (1995).
- [5] S.E. Harris, *Phys. Rev. Lett.* **77**, 5357 (1996).
- [6] G. Shvets and J.S. Wurtele, *Phys. Rev. Lett.* **89**, 115003 (2002).
- [7] A.G. Litvak and M.D. Tokman, *Phys. Rev. Lett.* **88**, 095003 (2002).
- [8] Mikhail Tushentsov *et al.*, *IEEE Trans. Plasma Sci.* **33**, 23 (2005).
- [9] E. Kawamori, *Plasma Phys. Controlled Fusion* **53**, 085015 (2011).
- [10] M.S. Hur, J.S. Wurtele, and G. Shvets, *Phys. Plasmas* **10**, 3004 (2003).
- [11] A. Yu. Kryachko, M.D. Tokman, and A.G. Litvak, *Nucl. Fusion* **44**, 414 (2004).
- [12] E. Kawamori, J.Y. Lee, Y.J. Huang, W.J. Syugu, S.X. Song, T.Y. Hsieh, and C.Z. Cheng, *Rev. Sci. Instrum.* **82**, 093502 (2011).
- [13] E. Kawamori, *Phys. Plasmas* **17**, 102108 (2010).
- [14] M. Fleischhauer and M.D. Lukin, *Phys. Rev. Lett.* **84**, 5094 (2000).